

Study of the Atomic Packing Fraction, Specific Surface Area and Morphology Index of Pure Titanium Dioxide Compound and Doped with Lead TiO_2 : Pb in Different Ratios



Ahmad Khoudro, Shaza Sater* and Duored Suliman*

Department of Physics, Tishreen University, Syria

Submitted: January 17, 2024; Published: March 12, 2024

*Corresponding author: Shaza Sater and Duored Suliman, Department of Physics, Tishreen University, Syria

Abstract

In this research, additional physical parameters were calculated for previous parameters that were set for samples of pure titanium oxide compound doped with lead in different proportions according to ($x = 0.2 - 0.5 - 0.7 - 0.9$ g) in its three phases (anatase, brookite and rutile) by making use of X-ray diffraction diagrams. XRD, where the computational results of the atomic packing fraction PF, the morphology index MI, and the specific surface area S showed the structural changes that occur to the pure powder as a result of doping it with different proportions of lead, so we have shown from the range to which the morphology index values belong that the compound belongs to pure titanium dioxide, and The values of the morphology index varied according to the different phases and the different doping ratios, and rutile had the largest value of MI at 0.2g Pd doping, and when calculating the specific surface area, the anatase phase appeared with the largest surface area compared to the other two phases at 0.7g Pd doping, then we explained the changes of the morphology index varies by parametric both the crystal size D on the one hand and the specific surface area S on the other hand. We also explained and explained the changes that appeared on the values of the atomic packing fraction of the compound after doping it with lead ratios.

Keywords: Powder; Morphology index; Titanium dioxide TiO_2 ; Doping; Lead Pb; Structural properties; Specific surface area; Physical properties; Atomic packing fraction

Introduction

The importance of our research comes from the importance of both the powders and the compound used, as the powders have a greater photocatalytic activity than the thin films of titanium dioxide, as well as the use of TiO_2 compound in many and wide applications, as titanium dioxide is a semiconductor used in photocatalysis [1] and in photovoltaic systems and dye-sensitive photocells [2,3], it has a large band gap $E_b = 3.2$ eV that makes this catalyst effective only in the ultraviolet region. These doping processes are: TiO_2 : SiO_2 [4], TiO_2 : N [5], TiO_2 : MgO [6], TiO_2 : PbO [7,8], TiO_2 : Pb [2,3,5,9-11]. TiO_2 also has a refractive index. It is high, which increases with increasing annealing temperature [12]. This compound also enjoys thermal and chemical stability, non-toxicity [13], its wide applications in optics and electronics [1-6,10,11,14-22], its biological and chemical inertness, and

its mechanical strength [23]. The titanium dioxide compound is characterized by three crystalline phases: anatase and rutile (tetragonal crystal system) and brookite (orthorhombic crystal system) as shown in Figure 1.

In this research, we calculated the atomic packing fraction P F, the morphology index MI, and the specific surface area S (m^2/g) of titanium dioxide compound doped with lead in different proportions, which we studied many of its physical properties previously using the X-ray diffraction device (XRD), where the diffraction charts enabled us For pure and lead-doped samples by calculating several physical values, including the values of crystal size D, cell size V, theoretical density $\rho_{(X\text{-ray})}$ and full width at half maximum intensity (FWHM), which we will use in this research to identify new values. New physical properties in order to enrich the investment of this compound in wider areas [24].

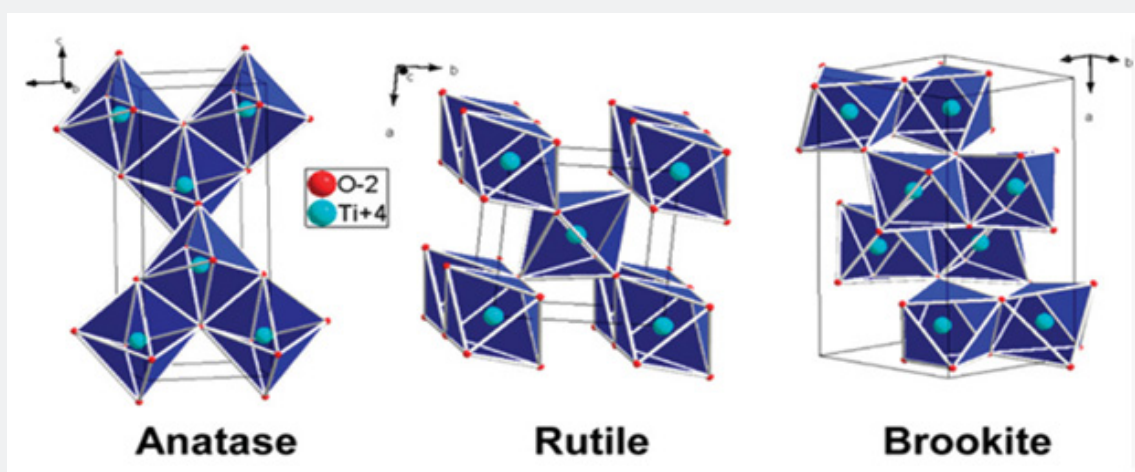


Figure 1: Crystal structure of TiO₂ rutile (tetragonal, P4₂/mmm), brookite (orthorhombic, Pbc_a) and anatase (tetragonal, I4₁/a) polymorphs [18].

Experimental Method

The process of preparing samples was carried out in the Faculty of Science at Tishreen University in the laboratories of the Departments of Physics and Chemistry. Pure and lead-doped TiO₂ powders in the proportions ($x = 0.2 - 0.5 - 0.7 - 0.9$) Ti_(1-x)Pb_xO₂ that we deal with in this research were previously weighed by a sensitive balance type (SARTORIUS) with an accuracy of gr (10-4). Which were manufactured by a solid-state interaction method [21] and [22] and were mixed and grinded well for two hours to become powders using an agate mortar and pestle, very fine, then sifted using a sieve. It has a hole size of 90 micron. Then, all samples were heated up to 200 °C by means of an incinerator.

Results and Calculation

Based on the values of crystal size D , cell size V , theoretical density $\rho_{(x\text{-ray})}$ and full width at half maximum intensity (FWHM) obtained from the reference study of the XRD plots [24] we were able to calculate the changes that occur To compact the atoms in the compound cell after we doped it with different dopant ratios, we calculated the packing fraction, or the so-called filling fraction, using the relationship (10) [25], which is equal to the ratio of the size of the atoms in the cell to The size of that cell:

$$P.F = \frac{V_P}{V} \quad (10)$$

P.F: atomic packing fraction

V_p : the size of the atoms present, which is equal to the number of oxygen atoms with the size of one atom n_1V_1 + the number of titanium atoms with the size of one atom n_2V_2 .

V : the cell size taken as (nm)³.

Considering the volume of an atom equals the volume of a sphere:

$$P.F = \frac{4}{3} \pi r^3, \quad \text{But } r = r_1 + r_2 \text{ and thereof :}$$

$$P.F = \frac{4}{3} \pi (r_1 + r_2)^3 \quad (11)$$

Where Z : the number of atoms per unit cell, which is equal to 2 in the rutile phase, 8 in the brookite phase, and 4 in the anatase phase.

r_1 and r_2 : the radius of the titanium atoms, Ti and O, respectively (Table 1).

Thus, the empty part of the titanium dioxide lattice appears according to Table 2.

We notice that in contrast to the increase in the cell size, the compaction coefficient decreased with the increase in the percentage of doping. It is clear that from the equation (10) that there is an inverse proportion between the cell size and the atomic packing fraction, while the latter is directly proportional to the size of the atoms in the compound, which differed according to the phase due to the difference in the number of atoms in the compound. Z unit cell between the three resulting phases. The highest value of the compaction coefficient was for the rutile phase $PF = 0.0596$, whose value was constant for all doped samples, due to the stability of the cell size of the doped samples in the rutile phase, where the crystal lattice constants of the rutile phase maintained their values by changing the doping ratios. As for the sample taken in phases together, the largest value of the packing

fraction was for the sample with the highest doping ratio 0.9g, but the cell size was the highest value and also the theoretical density had the lowest value at that value, which amounted to 4.069 g / cm^3 among the samples and The reason for this is only the significant decrease in density for the two phases of anatase and brookite,

which was greater for the stage of brookite in particular, and this corresponds to the increase in cell size for each of the previous two phases, knowing that the phase of brookite is the most present in the recombinant compound in this research (Figure 2).

Table 1: The atomic packing fraction of pure and lead-doped TiO_2 powders with ratios ($x = 0.2 - 0.5 - 0.7 - 0.9 \text{ g}$) taken for each phase separately and for the phases together.

Packing Fraction P.F					
The Products	Pure TiO_2	Pb: TiO_2 ($x=0.2\text{g}$)	Pb: TiO_2 ($x=0.5\text{g}$)	Pb: TiO_2 ($x=0.7\text{g}$)	Pb: TiO_2 ($x=0.9\text{g}$)
Rutile	0.0595	0.0596	0.0596	0.0596	0.0596
Anatase	0.0550	0.0550	0.0550	0.0550	0.0540
Brookite	0.0564	0.0563	0.0563	0.0563	0.0558
All phases	0.0570	0.0570	0.0570	0.0570	0.0565

Table 2: The blank fraction ratio of pure and lead-doped TiO_2 powders with ratios ($x = 0.2 - 0.5 - 0.7 - 0.9 \text{ g}$) taken for each phase separately and for the phases together.

Blank Fraction Ratio					
The Products	Pure TiO_2	TiO_2 : Pb ($x=0.2\text{g}$)	TiO_2 : Pb ($x=0.5\text{g}$)	TiO_2 : Pb ($x=0.7\text{g}$)	TiO_2 : Pb ($x=0.9\text{g}$)
Rutile	0.9405	0.9404	0.9404	0.9404	0.9404
Anatase	0.9450	0.9450	0.9450	0.9450	0.9460
Brookite	0.9436	0.9437	0.9437	0.9437	0.9442
All phases	0.9430	0.9430	0.9430	0.9430	0.9435

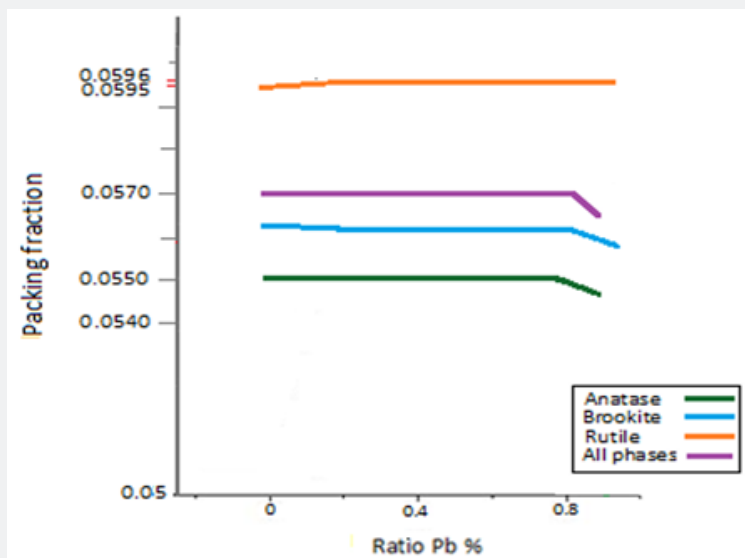


Figure 2: The atomic packing fraction PF of pure and lead-doped titanium dioxide samples at different ratios ($x = 0.2 - 0.5 - 0.7 - 0.9 \text{ g}$) in each of the anatase, brook it and rutile phases, and for both phases.

We note that the curves are closer by 99% to the curves that we obtained when drawing the theoretical density changes according to the dopant ratio, and this indicates the existence of a link between the density and the packing fraction, as it increases with the increase in density, and the increase in this fraction may indicate that the crystalline lattice of the samples has a preference. In the presence of repetition of the same crystal lattice (symmetry) with glide planes and screw axes that affect the cavities adjacent to it by installing bumps in the single molecular surface [15], where the lowest value of the packing fraction was 0.9 g, and the phase was the anatase phase, while the highest value of the packing fraction was for the rutile phase, in which all doping ratios are equal. The packing fraction is evaluated, and the increase in the packing fraction results in an increase in shear stress and an increase in optical conductivity. From the figure, the PF maintains a constant value for all pure samples. And the similarity to decrease when the doping ratio is 0.9 g, due to the increase in cell size and the decrease in the theoretical density. We can say that PF values fall within the range [0.0540-0.0550] for the anatase phase, within the range [0.0595-0.0596] for the rutile phase, within the range for the brookite phase [0.0558-0.0564]

and within the range for the whole compound [0.0565-0.0570]. The sample with an impurity ratio of 0.9 g was the most different from the pure sample in terms of the values of the PF.

Then we calculated the specific surface area S of pure and doped titanium dioxide powders for spherical granules using equation (11), as both equations (10) and (11) give us the same values for the specific surface area [15] and [16], respectively:

$$SSA = \frac{SA_{part}}{V_{part} * density} \quad (11)$$

$$S = \frac{6 * 10^3}{D \rho_{X-ray}} \quad (12)$$

S : the specific surface area is m^2/g .

V_{part} : particle size in nm^3 .

SA_{part} : surface area in nm^2 .

D : crystal size unit nm .

$\rho_{(X-ray)}$: The theoretical density of the X-ray diffraction spectrum for powders is g/cm^3 (Table 3).

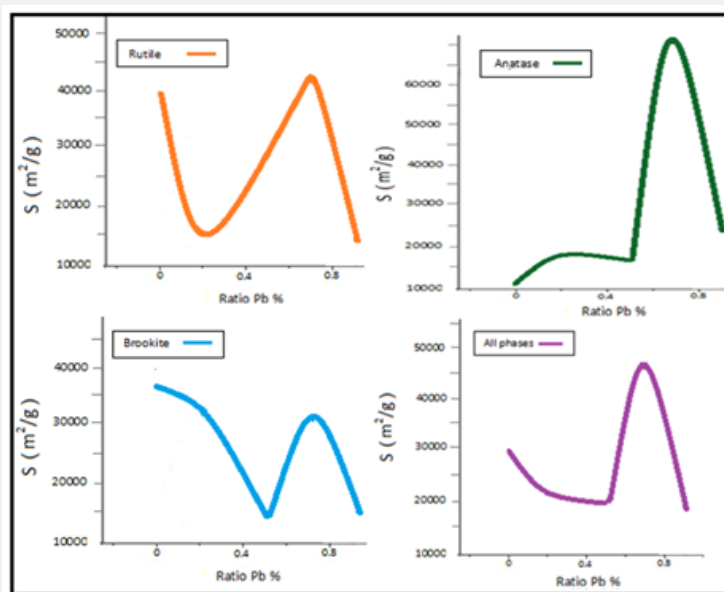


Figure 3: Specific surface area S (m^2/g) for pure and lead-doped titanium dioxide samples with different ratios ($x = 0.2 - 0.5 - 0.7 - 0.9$ g) in each of the anatase, brookite and rutile phases, and for both phases.

All samples are similar in the appearance of the graph in terms of increasing and decreasing the specific surface area at different dopant ratios, except for the anatase sample between the pure compound and the dopant with a ratio of 0.2 g. The graph shifts between them from decrease to increase (Figure 3). We note that

the surface-to-volume ratio decreases with the increase in grain size [14], meaning that the specific surface area decreases with increasing doping ratios, except for the percentage of lead doping that is equal to 0.7 g, at which the specific surface area increased due to the decrease in the grain size at this ratio only after its increase

in the rest. Lead doping ratios, as the study of the specific surface area allows us to identify the possibility of adsorption and non-homogeneous stimulation and the ability of the molecule to move and navigate on the surface and understand the interactions that occur on the surface or at the interface as the adsorption increases with the increase of the specific surface area and thus increases In homogeneous stimulation, among the surfaces of titanium dioxide compounds, it was found that the doping ratio is 0.7 g. The surface of the compound is active in the adsorption process due to its privilege of not saturating its atoms electronically despite the bonds formed by the atoms of this surface with neighboring atoms with ratios (x = 0.2- 0.5 - 0.7 - 0.9 g).

[18]. The values obtained are consistent with the researcher [19]. The specific surface area for both phases also fell within the range [47842.78 - 18191.06 m²/g], The anatase phase also had the highest value of the specific surface area compared to the other two phases, which amounted to S = 71061.38 m²/g because the size of its grains was the smallest for the inclusion ratio of g 0.7. S = 12948.71 m²/g, but the predominant phase of the compound, which is the brookite phase, has decreased the values of the specific surface area, giving us as a result a decrease in the values of the latter for the compound for all phases.

Table 3: Specific surface area of pure and lead-doped TiO₂ powders

S (m ² /g)					
The Products	Pure TiO ₂	TiO ₂ : Pb (x=0.2g)	TiO ₂ : Pb (x=0.5g)	TiO ₂ : Pb (x=0.7g)	TiO ₂ : Pb (x=0.9g)
Rutile	39803.97	16794.10	28846.96	42814.70	14064.61
Anatase	12948.71	18513.63	17333.94	71061.38	24710.20
Brookite	36586.95	30862.54	14834.62	29652.25	15798.35
All phases	29779.88	22056.76	20338.51	47842.78	18191.06

Table 4: Tabular figures giving the values of the morphology index for pure and lead-doped TiO₂ powders with the proportions (x = 0.2- 0.5 - 0.7 - 0.9 g).

Pure TiO ₂		TiO ₂ : Pb (x=0.2g)		TiO ₂ : Pb (x=0.5g)		TiO ₂ : Pb (x=0.7g)		TiO ₂ : Pb (x=0.9g)	
20 (deg)	MI (unit less)	20 (deg)	MI (unit less)	20 (deg)	MI (unit less)	20	MI (deg) (unit less)	20 (deg)	MI (unit less)
32.100	0.500	32.1	0.485	32.1	0.572	32.1	0.572	32.1	0.445
42.355	0.530	33.6	0.931	33.6	0.572	33.6	0.400	33.6	0.400
46	0.572	36.7	0.800	36.7	0.889	36.7	0.572	35.7	0.667
48.50	0.500	37.4	0.667	37.4	0.667	37.4	0.500	36.7	0.728
51.80	0.667	42.36	0.572	42.355	0.667	42.355	0.572	37.4	0.800
64.4	0.616	46	0.690	46	0.667	46	0.500	39.6	0.667
67	0.500	48.5	0.445	48.5	0.572	48.5	0.625	42.355	0.667
71	0.616	51.8	0.800	51.8	0.8	51.8	0.541	46	0.667
73.7	0.800	57.7	0.667	52.3	0.8	57.7	0.667	46.5	0.800
74.9	0.667	64.4	0.572	57.7	0.5	62.3	0.667	48.5	0.607
76.2	0.572	67	0.625	64.4	0.667	64.4	0.656	52.3	0.910
83	0.572	71	0.690	67	0.8	66.4	0.800	53.5	0.667
83.7	0.800	71.9	0.625	71	0.728	67	0.500	54.5	0.656
\overline{MI} For all phases	0.609	72.4	0.770	72.4	0.834	70	0.800	57.7	0.667
		73.7	0.690	73.7	0.770	71	0.500	61.215	0.785
	74.9	0.690	74.9	0.889	71.9	0.770	61.250	0.834	
	76.2	0.646	76.2	0.667	72.4	0.770	64.4	0.800	
	83	0.598	83	0.667	73.7	0.667	66.4	0.667	

	83.7	0.770	83.7	0.728	74.9	0.572	67	0.889	
	\overline{MI} For all phases	0.656	\overline{MI} For all phases	0.6892	76.2	0.667	70	0.834	
		83			79.5	0.667	71	0.667	
		0.500			0.800				
		71.9			0.800				
		83.7			0.667				
		0.800			0.667				
		72.4							
		\overline{MI} For all phases							
		0.6004							
		74.9							
		78.4							
		79.5							
		83							
		83.7							
		87.6							
		75							
		0.834							
		0.667							
		0.572							
		0.666							
		0.800							
							87.8	0.889	
								88.9	0.667
								\overline{MI} For all phases	0.712

Since the morphology index MI is related to both the particle size D and the specific surface area S, we calculated the MI for pure and lead-doped titanium dioxide powders using the equation (12) [20]:

$$M.I = \frac{FWHM_h}{FWHM_h + FWHM_p} \quad (13)$$

M.I: morphology index.

$FWHM_h$: The highest value of the full width at half the intensity (FWHM) measured in radians (rad).

$FWHM_p$: Full width values at half maximum intensity (FWHM) measured in radians (rad) (Table 4).

The range of MI for pure TiO₂ powder ranges within the range [0.500-0.800]. As for TiO₂ powder doped with lead, it belongs to the range [0.400-0.931], we notice that the range expands between the lowest and largest index values compared to the pure sample, and the rutile phase has the highest value of the morphology index. MI = 0.931 at 0.2 g lead impurity, followed by the value that we obtained in the sample impregnated with lead by 0.9 g to reach MI = 0.910. With an increase in lead impurity, there was a clear decrease in the width of the peaks, which was followed by an increase in the morphology index.

We note from Figures 4 & 5 that the average morphology index is directly proportional to the average crystal size of the phases

together \overline{D} which falls within the range [57.379-85.370 nm] and inversely proportional to the specific surface area S which falls within the range [47842.78 - 18191.06 m²/g] In this order, this agrees with the researcher [20]. The increase in the morphology index is due to the increase in the grain size due to the effect of lead impregnation, which caused the increase in the denominator of the relationship (13), which expresses the morphology index.

Conclusion

In this research, we completed the study of some physical properties of titanium dioxide compound doped with lead in different proportions, after studying the X-ray diffraction (XRD) patterns of anatase and rutile with a quadruple crystal system and brookite with a rhombic crystal system based in the compound in order to know the changes that occur in this compound and to increase Investing it in new and wide fields and applications, we have studied the atomic compaction coefficient, morphology index and specific surface area for each phase of the pure titanium dioxide compound doped with lead in different proportions, and we also took measurements for the phases together. The morphology index, which falls within the range [0.500-0.800], confirmed that the compound belongs to pure titanium dioxide, and the morphology index for the doped samples fell within the range [0.400-0.931], and its highest value belonged to the rutile

phase at the ratio of 0.2g, as it occurred. The specific surface area of the compound is within the range [47842.78 - 18191.06 m²/g], and the anatase phase had the highest value of the specific surface area compared to the other two phases, which amounted to S = 71061.38 m²/g. As for the atomic compaction ratio taken for the phases together, it fell within the range [0.0565- 0.0570]. The results were identical with many researchers.

References

1. Yu J, Yu JC, Cheng B, Zhao X (2002) Photocatalytic Activity and Characterization of the Sol-Gel Derived Pb-Doped TiO₂ Thin Films. *Journal of Sol-Gel Science and Technology* 24: 39-48.
2. Asahi R, Morikawa T, Ohwaki T, Aoki K, Taga Y (2001) Visible-Light Photocatalysis in Nitrogen-Doped Titanium Oxides. *Science* 293(5528): 269-271.
3. Yu J, Zhao X, Zhao Q (2001) Photocatalytic activity of nanometer TiO₂ thin films prepared by the sol-gel method. *J Mater Chem Phys* 69(1-3): 25-29.
4. Hu C, Tang YC, Yu JC, Wong PK (2003) Photocatalytic degradation of cationic blue X-GRL adsorbed on TiO₂/SiO₂ photocatalyst. *J Photocatal Appl Catal B Environ* 40(2): 131-140.
5. Hara K, Hariguchi T, Kinoshita T, Sayama K, Arakawa H (2001) Influence of electrolytes on the photovoltaic performance of organic dye-sensitized nanocrystalline TiO₂ solar cells. *J Sol Energy Mater* 70(2): 151-161.
6. Bandara J, Hadapangoda CC, Jayasekera WG (2004) Jayasekera WG TiO₂/MgO composite photocatalyst: the role of MgO in photoinduced charge carrier separation. *J Appl Catal B Environ* 50(2): 83-88.
7. Daniele S, Papiernik R, Hubert PLG, Jagner S, Hikansson M (1995) Single-Source Precursors of Lead Titanate: Synthesis, Molecular Structure and Reactivity of Pb₂Ti₂(μ₄-O)(μ₃-O-i-Pr)₂(μ₂-O-i-Pr)₄(O-i-Pr)₄. *Inorg Chem* 34: 628-632.
8. Hubert PLG, Daniele S, Papiernik R, Massiani MC, Septe B (1997) Solution routes to lead titanate: synthesis, molecular structure and reactivity of the Pb-Ti and Pb-Zr species formed between various lead oxide precursors and titanium or zirconium alkoxides. Molecular structure of Pb₂Ti₂(μ₄-O)(OAc)₂(OPri)₈ and of PbZr₃(μ₄-O)(OAc)₂(OPri)₁₀. *J Mater Chem* 7(5): 753-762.
9. Cheng SD, Kam CH, Zhou Y, Que WX, Lam YL, et al. (2000) Sol-gel derived nanocrystalline thin films of PbTiO₃ on glass substrate. *Thin Solid Films* 375(1-2): 109-113.
10. Fujishima A, Rao TN, Tryk DA (2000) Titanium dioxide photocatalysis. *Journal of Photochemistry and Photobiology C: Photochemistry Reviews* 1(1): 1-21.
11. Zeng X, Liu Y, Wang X, Yin W, Wang L, et al. (2002) Preparation of nanocrystalline PbTiO₃ by accelerated sol-gel process. *Materials Chemistry and Physics* 77(1): 209-214.
12. Krishna KM, Rahman MM, Miki T, Soga T, Igarashi K, et al. (1997) Optical properties of Pb doped TiO₂ nanocrystalline thin films: A photoluminescence spectroscopic study. *Applied Surface Science* 113-114: 149-154.
13. Eliana P, Vittorio L, Torres MF, Sham E (2015) Nitrogen doped TiO₂ photoactive in visible light. *Revista* 11624: 561-570.
14. Chen J, Yaling Li, Wang Y, Yun J, Cao D (2004) Preparation and characterization of zinc sulfide nanoparticles under high-gravity environment. *Mat Res Bull* 39(2): 185-194.
15. Rutherford JS (2005) Vander Waals Bonding and Inert Gases. *Encyclopedia of Condensed Matter Physics*.
16. Jiji A, Joseph N, Donald RB, Daniel M, Amit S, et al. (2006) Size-Dependent Specific Surface Area of Nanoporous Film Assembled by Core-Shell Iron Nanoclusters. *J Nanomater* 54961: 1-4.
17. Yong PJ, Yun JL, Ki WJ, Jin OB, Dae JY (2006) Chemical Synthesis and Characterization of Highly Oil Dispersed MgO Nanoparticles. *J Ind Eng Chem* 12(6): 882-887.
18. Zhang J, Xiao X, Nan J (2010) Hydrothermal-hydrolysis synthesis and photocatalytic properties of nano TiO₂ with an adjustable crystalline size. *J Hazardous Mat* 176(1-3): 617-622.
19. Damien D, Belharouak I, Amine K (2010) Tailored Preparation Methods of TiO₂ Anatase, Rutile, Brookite: Mechanism of Formation and Electrochemical Properties. *American Chemical Society* 22(3): 1173-1179.
20. Theivasanthi T, Alagar M (2011) An Insight Analysis of Nano sized powder of Jackfruit Seed. *Nano Biomed Eng* 3(3): 163-168.
21. Thirugnanasambandan T (2012) Titanium dioxide (TiO₂) Nanoparticles - XRD Analyses - An Insight.
22. Primo A, García H (2013) Solar Photocatalysis for Environment Remediation. In: Suib SL, *New and Future Developments in Catalysis*, chapter 6, Amsterdam, Elsevier, USA.
23. Mehdizadeh P, Tavangar Z, Shabani N, Hamadani M (2020) Visible Light Activity of Nitrogen-Doped TiO₂ by Sol-Gel Method Using Various Nitrogen Sources. *J Nanostruct* 10(2): 307-316.
24. Sater S, Khoudro A, Dalla A (2023) Studing Some of Physical Properties OF a Lead Doping Titanium Dioxide TiO₂: Pb with Different Ratios. *Physical Science & Biophysics Journal* 7(1).
25. Patiño WFO, Estrada N (2020) Densest arrangement of frictionless polydisperse sphere packings with a power-law grain size distribution. *Granular Matter*, Verlag GmbH Germany, part of Springer Nature.



This work is licensed under Creative Commons Attribution 4.0 License
DOI: [10.19080/JOJMS.2024.08.555740](https://doi.org/10.19080/JOJMS.2024.08.555740)

**Your next submission with JuniperPublishers
will reach you the below assets**

- Quality Editorial service
- Swift Peer Review
- Reprints availability
- E-prints Service
- Manuscript Podcast for convenient understanding
- Global attainment for your research
- Manuscript accessibility in different formats
(Pdf, E-pub, Full Text, Audio)
- Unceasing customer service

Track the below URL for one-step submission

<https://juniperpublishers.com/submit-manuscript.php>